Novel microfabricated Pd–Au/SiO_2 bimetallic model catalysts for the hydrogenation of 1,3-butadiene

A.C. Krauth [a], G.H. Bernstein [b] and E.E. Wolf [a,*]

Departments of Chemical Engineering [a] and Electrical Engineering [b], University of Notre Dame, Notre Dame, IN 46556, USA

Received 24 October 1996; accepted 4 March 1997

Model Pd–Au/SiO_2 bimetallic catalysts were prepared via a microfabrication method and their catalytic activity for the hydrogenation of 1,3-butadiene was compared with thin film catalysts. The microfabricated catalyst consisted of Pd–Au squares with various surface compositions, approximately 4 μm in size and separated by 4 μm on a silica/silicon support. The main advantage of the microfabricated bimetallic catalysts is that alloy formation is guaranteed and XPS results showed that surface segregation occurred for the Au-rich compositions. The apparent activation energies of the bimetallic catalysts were lower than that of the pure Pd catalyst with a minimum occurring at $\sim$ 65 at% Pd. The bimetallic catalysts, however, have fewer active Pd sites, hence the conversions are comparable. The microfabricated catalysts were more active than the thin film samples, because the thin film samples showed evidence of a high degree of sintering after pretreatment, unlike the microfabricated catalysts in which sintering did not occur.

Keywords: microfabricated catalysts, bimetallic, Pd–Au/SiO_2, hydrogenation of 1,3-butadiene

1. Introduction

Bimetallic catalysts are used in many catalytic processes in the chemical and petroleum industry. A few important examples include Pt–Re, Pt–Sn, and Pt–Ir on γ-alumina for catalytic reforming, and the Pt–Pd–Rh three-way catalyst used in an automobile's catalytic converter [1]. Most bimetallic catalysts are very sensitive to the preparation procedure and there are many factors, such as particle size, composition and structure, that dictate the actual activity of the catalyst. For a bimetallic catalyst on a high-area support, there is no certainty that the catalytic metals are going to interact to form an alloy. Even when it is determined that an alloy has been formed, there are further questions concerning its composition and surface structure. In many systems there is some degree of surface segregation and often the surface composition and bulk composition vary widely [2], which is further complicated by particle size effects. For example, Alerasool and Gonzalez [3] found that for a silica-supported Pt–Ru catalyst the larger particles were rich in Pt while the smaller ones were Ru-rich. For most bimetallic catalysts their activity and selectivity reflect a statistical average of particles with different sizes, composition and structure which is related to the preparation procedure leading to such averages.

In an attempt to define completely the size and composition of each particle, we used a microfabrication technology to prepare bimetallic Pd–Au model catalysts. The advantage of this methodology is that a catalyst can be prepared in a predesigned manner, which is specially relevant for bimetallic catalysts. Small wells are actually etched into the support and thin films of each metal are deposited into these wells. This guarantees interaction between the two metals, unlike other preparation procedures. Microfabrication technology was developed in response to the needs of the microelectronics industry, for the purpose of placing millions of devices on a single chip [4]. Other applications of this technology have already appeared in the area of solid-state catalytic gas sensors [5]. In the area of catalysis, Zuburtikudis and Saltsburg [6] have used this methodology to mimic size effects in supported metal catalysts. Previous work done in our group in preparing a microfabricated catalyst [7] is the basis for the work presented in this paper. Using this methodology we prepared a model supported bimetallic catalyst, wherein the size, spacing and composition of each well containing the two metals are determined a priori and the same for each well.

The main disadvantage of the microfabricated catalyst is that it has a low surface area as compared to a conventional industrial catalyst; however, the main objective of this work is to study compositional effects in bimetallics with this new unexplored method of catalyst preparation.

Pd and Au were chosen for this work, because they have been extensively studied, as evident by the number of reviews published [8–11], their solid solutions are almost completely miscible [12], and the system could not exhibit surface segregation. This last point, however, has been the source of some controversy. Maire et al. [13] reported that since there is little difference in the heat of vaporization for Pd and Au (90 kcal/mol to 88 kcal/mol, respectively), surface tensions (1430 erg/cm^2 to 1340 erg/cm^2, respectively), atomic diameters (2.74 Å to 2.88 Å, respectively) and sputtering yields at 500 eV Ar^+

* To whom correspondence should be addressed.

(2.1 atoms/ion to 2.4 atoms/ion, respectively), there should be very little surface enrichment. Indeed, some authors state that they were not able to detect any significant surface enrichment in this system [14–16]; however, others have reported that there is a significant enrichment in Pd or Au. The variability in results is due partly to the different methods used to prepare the samples. Oxygen treatment [13] or sputtering [17] tends to enrich the surface in Pd; whereas, annealing the sample in vacuum after cleaning [17,18] increases the surface composition of Au. The important point is that the occurrence of surface enrichment depends on the method of preparation and must be confirmed experimentally.

The catalytic activity of the microfabricated catalyst was evaluated during the hydrogenation of 1,3-butadiene, because reasonable conversions have been reported with other model, low-area thin film monometallic catalysts [19–23]. Butane, 1-butene, cis-2-butene and trans-2-butene are the four reaction products. The same reaction was studied by Joice et al. [24] on Pd–Au/pumice prepared by precipitation of Pd and Au chlorides. These authors found that the activation energy remained fairly constant at $\sim$ 10.5 kcal/mol over the range 0–60% Au (atomic percentage) and then increased to $\sim$ 15 kcal/mol at 65–70% Au and decreased to $\sim$ 9.2 kcal/mol at higher Au compositions. The constant activation energy with varying Pd compositions suggests that an alloy was not formed. Miura et al. [25] studied the same reaction on an egg-shell type Pd–Au/Al_2O_3 catalyst. The addition of Au lowered the Pd activity. At higher conversions ($>$ 30%) the bimetallic catalyst was more selective towards 1-butene, and less to butane, than the Pd catalyst. The formation of the 2-butenes was not significantly affected by the presence of Au.

The objectives of this work focus mainly on the effect of alloy composition on the kinetics of the reaction and not on particle size effects, or on the suitability of this model catalyst to be as active as supported catalysts. The results are compared with those obtained on thin film catalysts, as well as with results reported by others on supported bimetallic catalysts.

2. Experimental

2.1. Catalyst preparation

The preparation of a microfabricated monometallic Pd catalyst was described in detail in an earlier paper [7], thus it will only be outlined here emphasizing mainly the bimetallic preparation. The silica support was obtained by oxidizing a clean, n-type, $\langle 100 \rangle$ silicon wafer. The selected pattern for the catalytic islands consisted of 4 μm squares separated by 4 μm of silica on each side. The size of these wells, which is imposed by the contact lithographic technique used, is orders of magnitude larger than crystallites in supported catalysts. For this reason only compositional effects are emphasized in this work. When each well is filled with the two metals, they form a pattern of square metallic islands on the surface. To form the pattern, a positive photoresist was applied to the surface of the wafer and brought into contact with a glass photomask with a grid of square openings imprinted on it. After exposure and development of the photoresist layer (see ref. [7] for details), the resulting layer consisted of wells exposing the SiO_2 support. The wafer was then immersed in a 5% buffered hydrofluoric acid for 15 s to etch part of the exposed silica, thereby transferring the pattern, etched approximately 250 Å into the SiO_2 surface into which the catalytic particles were deposited by evaporation.

Palladium (99.997% pure, Johnson Matthey AESAR/ALFA) was deposited onto the wafer via a vacuum thermal evaporator (VEECO VES 7700). The chamber was evacuated to $(2–4)\times10^{-7}$ Torr and a slowly increasing current, reaching a maximum of 40 A, through a tungsten wire basket evaporated 30.2 mg of Pd with an estimated film thickness of approximately 200 Å. Then an Au film (99.99+% pure, Material Research Corp.) of the required thickness to yield the desired bimetallic bulk concentration was deposited using a vacuum electron-beam evaporator (AIRCO Temescal FC-1800). After reaching a chamber pressure of $(4–6)\times10^{-7}$ Torr, the e-beam current was set to achieve a deposition rate of approximately 5 Å/s. After depositing the two metals, the wafer was immersed in acetone, to dissolve the remaining photoresist and the metal on top of the resist. Thus, the metal that remained filled the square wells previously opened in the silica layer. The wafer was then cut into sections of 1.2×0.5 cm to accommodate it in the reactor. The samples thus prepared were placed in the reactor and pretreated with a procedure adopted after several studies showing that alloy formation took place.

Pd–Au thin film catalysts were also prepared for the purpose of comparison with the microfabricated catalysts. The same SiO_2/Si wafer was used as a support for the thin film samples. The Pd film and the Au film were deposited using the same techniques and processing parameters used for the microfabricated catalysts, but without the lithographic process. Except for the photomasks, the microfabricated catalysts were prepared in the Microelectronics Laboratories in the Electrical Engineering Department at the University of Notre Dame.

2.2. Catalytic activity measurements

The hydrogenation of 1,3-butadiene was carried out in a quartz tubular reactor at atmospheric pressure, which was heated by an electrical heating jacket and the temperature was kept constant by a temperature controller. The catalysts were reduced in situ in a hydrogen flow of 20 cm^3/min for 6 h at 450°C. The flow of reac-

tants introduced into the reactor consisted of hydrogen (partial pressure of 500 Torr), 1,3-butadiene (4 Torr) and nitrogen to produce a constant flowrate of 110 cm^3/min. Ultra-high purity grade nitrogen and hydrogen were used and the 1,3-butadiene has a 99.5% purity (Matheson Gas Products). The catalyst was exposed to hydrogen flow until the desired reaction temperature was achieved. Then the flow was switched to the reaction mixture and several samples of the product stream were taken. After sampling at a given set of reaction conditions, to avoid any possible deactivation effects, the catalyst was exposed to pure hydrogen flow until the next set of conditions was attained. The reaction products were analyzed using a Hewlett Packard (series 5710A) flame ionization detector (FID) and separated by a 7 foot chromatographic column packed with 0.19% picric acid/graphpac packing (Alltech Associates, Inc.).

2.3. Catalyst characterization

Several techniques were used to characterize the size and composition of the microfabricated catalysts. The catalytic surface was characterized with atomic force microscopy (AFM) to obtain information on the surface microstructure and X-ray electron spectroscopy (XPS) to measure surface composition. The AFM used in this study is a commercial Nanoscope II system (Digital Instrument Inc.) operating in air. A scan head with an 8000 nm range and a silicon nitride tip was utilized. The AFM was operated in the height imaging mode with a setpoint voltage between 0 and 1.6 V at ambient conditions. All of the AFM images presented herein were taken after the sample had been alloyed using the high temperature pretreatment, but before they were exposed to the reaction mixture. At the resolution used, the reacted samples did not exhibit significant morphological changes and, thus, are not shown. Three separate areas of the catalyst were scanned to ensure that the images were representative of the whole sample.

The XPS results were obtained in a spectrometer (Kratos Analytical Inc.) using monochromatic Mg Kα radiation ($h\nu = 1253.6$ eV). The base pressure of the instrument is 1×10^{-9} Torr. The C 1s peak position was assigned to 284.6 eV to calibrate the electron binding scale energies. All surface compositions were calculated using the total area under the Pd $3d_{3/2}$ and Pd $3d_{5/2}$ peaks and Au $4f_{5/2}$ and Au $4f_{7/2}$ peaks, along with their corresponding sensitivity factors (5.356 and 6.250, respectively).

Characterizing the samples with X-ray diffraction was attempted, but the metallic films were too thin to yield detectable coherent diffraction patterns. Due to the small surface area of the microfabricated catalyst, chemisorption measurements by pulse flow techniques were not sensitive enough to yield reliable results.

3. Results and discussion

3.1. XPS results

The catalysts were pretreated in different gases and at different temperatures to establish the proper conditions at which the two metal layers interdiffuse to form an alloy. A sample with a nominal bulk composition of 85 at% Pd was split into three sections, and each piece was treated for 12 h at 450°C in a flow of either air, hydrogen, or nitrogen. The composition of the samples was then measured by XPS. Because of the presence of SiO_2 in between the islands, the atomic ratio between Au or Pd to the sum of the two metals obtained from the XPS data is taken as the surface composition of each island (thus excluding SiO_2). XPS actually samples the first 2–3 atomic layers, consequently the values reported represent an average within this near-surface region. The XPS results showed that the sample treated in air at 450°C had a surface comprised entirely of palladium oxide, whereas the other two samples treated at the same temperature in hydrogen and nitrogen exhibited nearly identical surface compositions (84 at% Pd for the nitrogen treated sample and 87 at% Pd for the hydrogen treated sample) with no PdO detected. The agreement between bulk and surface composition for this sample proves that an alloy was indeed formed, otherwise only Au would be detected by XPS since the Au layer was deposited on top of the Pd layer. Consequently, the H_2 pretreatment was selected for alloying the samples, since this guarantees that Pd is in its metallic state. A sample treated for 6 h gave the same XPS surface composition as those treated by 12 h, hence all subsequent samples were treated for 6 h. In reality, a much shorter alloying time would still have ensured surface equilibrium. Work reported by Jablonski and coworkers [17] demonstrated that surface equilibrium of Pd–Au foils is reached within 1.4 h at 400–600°C. The longer pretreatment time adopted in this study is for the benefit of complete reduction of Pd.

Six samples of different composition were prepared for the remainder of the study. The monometallic Au catalyst exhibited no catalytic activity at any temperature below 250°C and thus was not studied further. For the other five samples the amount of metal deposited, the estimated bulk composition, and the surface composition as determined by XPS are shown in table 1. The *Pd-rich* samples have surface compositions that nearly match their estimated bulk Pd concentration, differing only by a couple of percent from the XPS values, with no evidence of any significant surface segregation. In the *Au-rich* samples, however, surface segregation was observed. For example, for an equal atomic concentration of Pd and Au, the surface is richer in Pd by 14%, and as the bulk concentration of Au begins to dominate, the surface segregation of Pd increases. The surface of the sample with an estimated bulk composition of 25 at% Pd

Table 1
Characterization of the Pd–Au/SiO_2 catalysts

Type	Pd thickness [a] (Å)	Au thickness [b] (Å)	Bulk comp. [c,d] (% Pd)	Surface comp. [c,e] (% Pd)	% increase in Pd
fabricated	177	613	25	44	76
fabricated	197	231	50	57	14
fabricated	204	80	75	73	−2.6
fabricated	192	37	85	87	2.4
fabricated	137	0	100	100	0.0
thin film	208	244	50	54	8.0
thin film	209	82	75	76	1.3

[a] From calibration curve of thermal evaporation.
[b] From calibration curve of e-beam evaporation.
[c] Composition is defined as ratio of Pd to total amount of metal.
[d] From the atomic ratio Pd/(Pd + Au).
[e] From XPS.

yields a Pd surface composition of 44 at%, a 76% increase in Pd concentration. The general trend is that the richer the bulk is in Au, the greater the surface enrichment of Pd in relation to the bulk values. From this point on, each catalyst will now be referenced by the XPS measurements, since these results reflect better the surface composition. The thin films also exhibited the same trend as the microfabricated catalysts (also shown in table 1). Both samples (50 at% bulk Pd and 75 at% bulk Pd) showed evidence of Pd surface enrichment (54 at% Pd and 76 at% Pd, respectively).

There is some uncertainty in the literature as to the state of the surface of a Pd–Au alloy as compared to the bulk. Our results show surface enrichment by Pd may be a direct result of the hydrogen treatment, because hydrogen is soluble in Pd and this affinity will draw Pd to the surface [13]. Jablonski and coworkers [17] reported surface segregation when the surface of their samples became enriched in Au after annealing and cleaning in *vacuum*. Clearly, the presence of surface segregation depends on the gas atmosphere and the pretreatment used. For our catalysts, pretreated in hydrogen, the surface enriches in Pd and the enrichment increases as the bulk Au concentration increases.

3.2. AFM characterization

The surface morphologies of the catalysts imaged by AFM are displayed in figure 1 showing 1000 nm $\times$1000 nm areas of *one* catalytic island. The morphology of the islands consists of smaller grains or particles. The pure Pd sample, shown in figure 1a, has grains with a columnar structure with an average size of 140 nm. The surface roughness for this catalyst (1.16 nm^2/nm^2 of geometric area) is higher than any other sample as determined by the Nanoscope II surface roughness program. The sample with 73 at% surface Pd (figure 1b), exhibits a completely different surface morphology. The average particle size seen in the islands of this catalyst is the largest of any of the bimetallic catalysts at 160 nm, with a surface roughness of 1.08 nm^2/nm^2 of geometric area, and a surface comprised of hills and trenches. The three remaining catalysts have surface structures similar to the one shown in figure 1c corresponding to the 87% Pd catalyst, with no unique features to distinguish between them at the resolution used in these micrographs. Each of the three samples has islands with particles with an average size of 70–100 nm and a surface roughness of 1.01–1.04 nm^2/nm^2 of geometric area. Attempts were made to increase the resolution, but the limitations of the AFM (versus STM) in imaging rough surfaces did not yield relevant images at higher resolution.

AFM images of the 76 at% Pd and 54% Pd thin film catalysts are shown in figure 2. These images show that the thin film catalysts experience a high degree of sintering during the hydrogen pretreatment that is not seen in the microfabricated catalysts. The same effect also occurs in the 54 at% Pd thin film catalyst. Apparently, the deposition of the two metals into the 4 micron wells in the microfabricated catalysts seems to anchor the metal into the wells and suppresses the movement of metal atoms across the surface. In the microfabricated catalyst the metal is trapped in a fixed volume without the degree of mobility existing in the thin film catalysts. Thus, due to sintering, the *total* number of Pd surface atoms available in the thin film catalysts is less than in the microfabricated catalysts, even though they have the same Pd/Au surface ratio.

3.3. Catalytic activity

Kinetic results were obtained in the temperature range 21–50°C to achieve differential conversions to obtain Arrhenius plots for each catalyst. The selectivity towards butane for each catalyst was negligible, hence it was assumed that one mole of hydrogen reacted with one mole of butadiene. This was important, because the rate of hydrogen consumption needed to be expressed as a function of butadiene conversion to calculate the rate constant. Also, since the catalyst was in the form of a

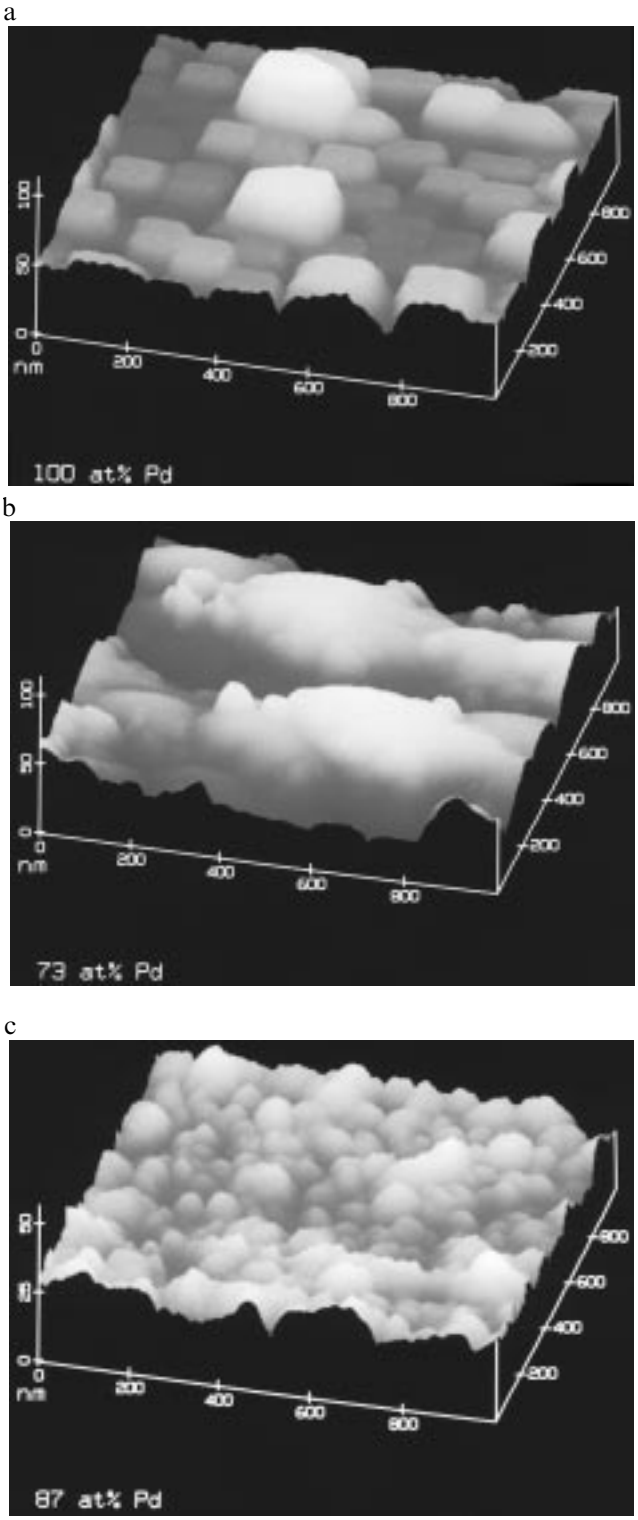

Figure 1. AFM images (1000 × 1000 nm^2) of the surface of an island of the microfabricated catalysts; (a) 100% Pd, (b) 73 at% Pd–27 at% Au, (c) 76 at% Pd–24 at% Au thin film.

wafer, the reactor was assumed to approximate a differential reactor. Once the rate was determined, the rate constant was calculated assuming that the reaction was zero order in butadiene and first order in hydrogen, as it was demonstrated in a previous study by Joice and coworkers [24]. The Arrhenius plots for all the microfabricated samples are shown in figure 3a and, for the sake of comparison, the 57 at% Pd microfabricated catalyst is compared to the 54 at% thin film catalyst in figure 3b. The apparent activation energies and the pre-exponential factors, are listed in table 2. It is interesting to note that the 57 at% Pd catalyst has the highest rate constant at room temperature (490 $cm^3/(g\text{-}Pd\ s)$), while the pure Pd sample has a rate constant at room temperature (67.5 $cm^3/(g\text{-}Pd\ s)$) that is lower than any of the samples, except for the 44 at% Pd catalyst. The highest activation energy measured corresponds to the pure Pd sample (20.0 kcal/mol) and it decreases to a minimum at 65% Pd surface concentration before increasing again. The 73 at% Pd catalyst has the lowest preexponential factor which contributes to a lower rate than samples with lower and higher composition. This catalyst also has a smoother surface morphology than any of the other samples (figure 1c) which could play a role in its lower activity. The trend in the change in activation energy with Pd composition is that it reaches a minimum as Pd composition decreases. This minimum is bounded by the activation energy of pure Pd and that of pure Au, which is rather high and outside the experimental temperature range studied. The two thin film catalysts exhibit values for the activation energy similar to those of the microfabricated catalysts, demonstrating the reproducibility of the measurements. These activation energies were lower than the value for the monometallic Pd catalysts. As the catalysts become richer in Au, the activation energy increases again towards the value of pure Au, hence the minimum.

The previous rate constants are based on the estimated weight of Pd deposited. A turnover frequency (TOF) based on the estimated number of surface Pd atoms can also be calculated using the XPS information on surface composition, the geometric area, and the surface roughness factors provided by the AFM images. In these estimates, Au atoms are assumed inactive, as was shown by the pure Au catalyst, hence the area of Au is not accounted as active area. The TOFs of the five catalysts at 21°C are also listed in table 2. The TOFs for the microfabricated catalysts at room temperature range from a low of 8.4 s^{-1} for the pure Pd catalyst to a high of 176.5 s^{-1} for the 57 at% Pd catalyst. The TOFs of the Pd microfabricated catalyst can be compared to TOFs reported for Pd single crystals. The most active face of Pd (Pd(110)) has a TOF of 24 s^{-1} at 27°C [26], which is an order of magnitude greater than the TOF reported for Pd(111) face [26]. The same group reports [26] that Pd/SiO_2 has about the same activity as Pd(111), with a TOF of 3 s^{-1} at 27°C. The pure Pd microfabricated catalyst has a TOF of 17.5 s^{-1} at 27°C, which suggests that the activity of this catalyst is bounded by the two extremes of the low angle index orientations. One interpretation of these results is that in the Pd microfabricated catalyst

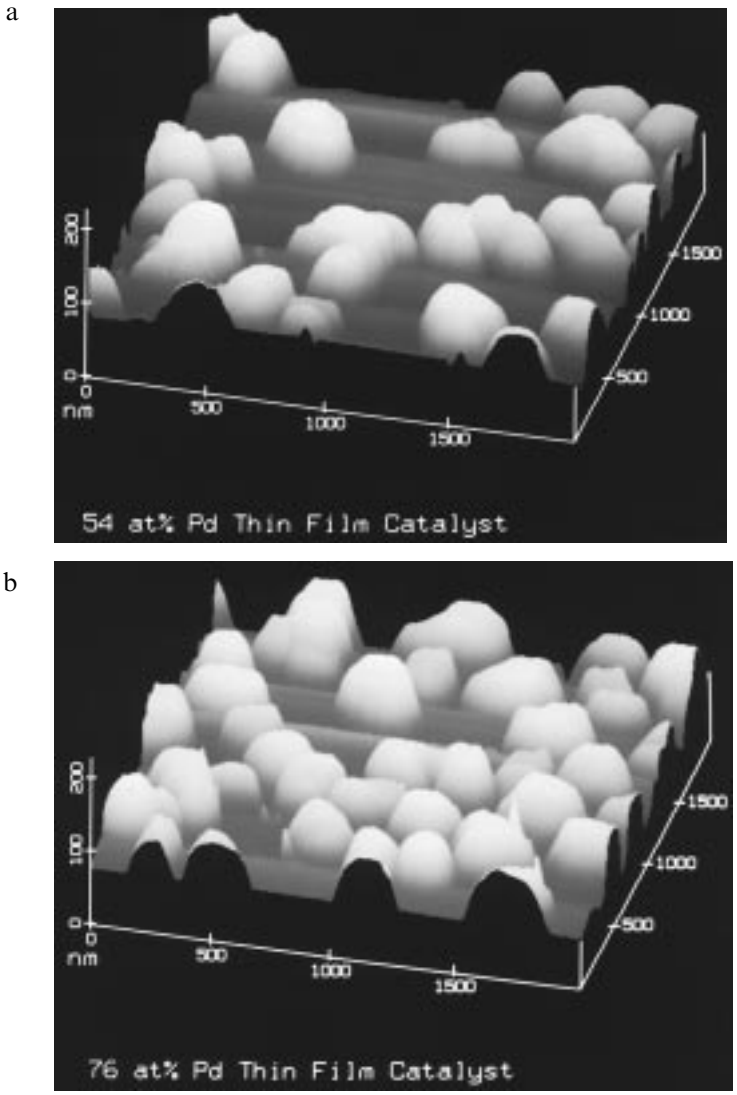

Figure 2. AFM images (2000 × 2000 nm^2) of the surface of thin film catalysts; (a) 54 at% Pd–46 at% Au, and (b) 76 at% Pd–24 at% Au thin films.

the surface is a composite of orientations that lies between that of Pd(110) and Pd(111). We attempted to characterize the crystal faces present in the microfabricated catalyst, but we were not able to obtain a signal from XRD even when using a grazing angle technique. So due to the experimental difficulty in determining the surface structure of the polycrystalline thin islands we are not able to prove the above conjecture. The kinetic results indicate that the sites created by alloy formation although fewer, are more active than the pure Pd catalyst.

The butadiene conversion for each catalyst as a function of temperature, in a range from 60 to 220°C, is displayed in figure 4. At higher temperatures, i.e. 220°C, the monometallic Pd sample converts more butadiene (61%) than any of the bimetallic catalysts which range from 54% (87 at% Pd) to 45% (73 at% Pd). This reflects the different activation energy of the various samples as well as transport effects. At higher temperatures (> 60°C) the TOFs no longer reflect the true activity of the Pd atoms, since mass and heat transfer become important. An estimate of the Damkohler number (Da) for this reaction at temperatures above 60°C show that the Da lies between 15 and 25, depending on the composition of the catalyst. This affects the conversion which now results from a combination of kinetics and transport effects.

The activities of the two thin film catalysts are also shown in table 2. For the 76 at% Pd thin film and for the 73 at% Pd microfabricated catalysts the activation energies are nearly the same (6.38 and 6.52 kcal/mol respectively). Likewise, the 54 at% Pd thin film catalyst has an activation energy of 5.97 kcal/mol as compared to 5.84 kcal/mol for the 57 at% Pd microfabricated catalyst. These results agree well with the fact that the compositions of the thin films and microfabricated catalysts

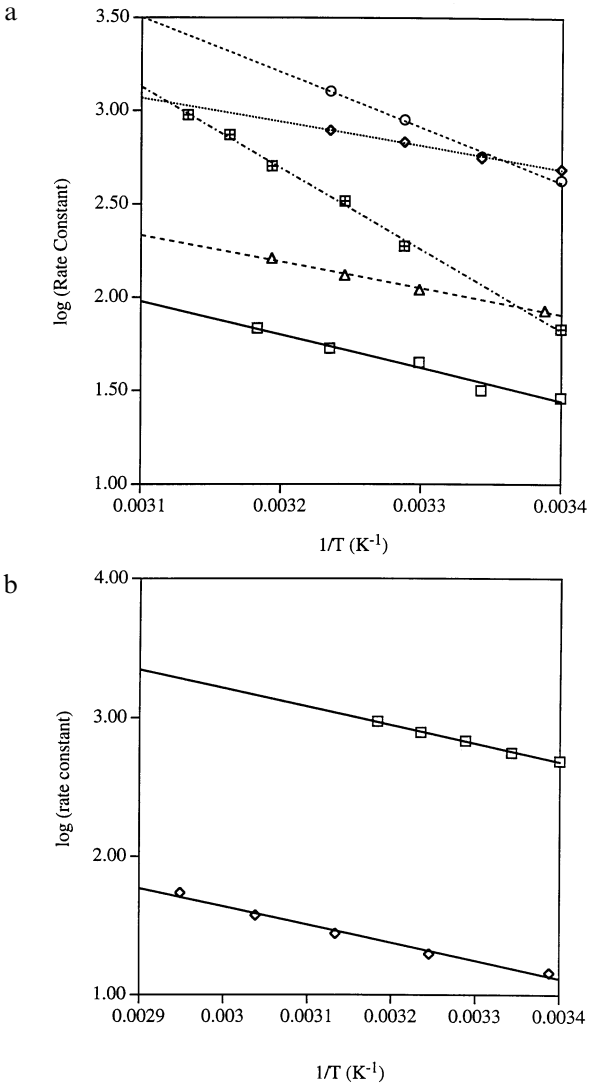

Figure 3. Arrhenius plot of rate constants for the hydrogenation of 1,3-butadiene over (a) Pd–Au/SiO_2 microfabricated catalysts; (□) 44 at% Pd, (◇) 57 at% Pd, (△) 73 at% Pd, (○) 87 at% Pd, (⊞) 100 at% Pd, and (b) (□) 57 at% Pd microfabricated catalyst and (◇) 54 at% Pd thin film catalyst. Reaction conditions: $P_{tot} = 1$ atm, $H_2/C_4H_6 = 125$, total flow = 110 cm^3/min.

are nearly the same. The main difference between the thin film and microfabricated catalysts is that the latter are more active and have higher reaction rate constants as demonstrated by their Arrhenius plots. The reason for the increased activity cannot be attributed to the 4 micron particle sizes in the microfabricated catalysts, since this is far too large to be due to any particle size effect. Work done by Tardy et al. [22] demonstrates that Pd particles larger than 2.8 nm behave similarly to bulk palladium for this reaction. Whereas the microfabricated and thin film catalysts have the same surface metal composition, the morphology of the pretreated surface is significantly different in both catalytic systems. The AFM results show that after pretreatment, the thin film catalysts experience significant sintering and three-dimensional growth, whereas each island in the microfabricated catalysts retains its two-dimensional morphology. Thus after pretreatment, the total number of Pd atoms exposed to the reactants is higher in the microfabricated catalysts than in the thin films, which is reflected in the difference in the overall activity. The results showing the sintering of the Pd thin film catalysts (figure 2) and the lack of sintering of the microfabricated catalysts (figure 1) are fairly clear from the AFM micrographs. In the microfabrication process the Pd–Au islands are actually embedded into a well in the SiO_2 support which constrains their movement.

The advantage of increased control over alloying in the microfabricated catalyst demonstrated by the kinetic data was not evident from earlier work. Joice and coworkers [24] reported that the addition of Au did not significantly change the activation energy of the reaction, indicating a lack of alloying, until they reached 65–70 at% Au. However, no evidence was reported of whether a true alloy had been formed, or if the metals had nucleated at separate sites. Miura et al. [25] used EPMA analysis to confirm that the distribution of Au and Pd was uniform within the pellet; but they did not report much kinetic data. The microfabrication technique guarantees that the two metals are in contact in the same place, and XPS and the activation energy data confirmed that an alloy was formed. If the Pd and Au had formed separate phases on the surface, the activation energy would have remained constant over the range of compositions. One can speculate that the filling of the Pd 4d-band leads to the decrease in activation energy from pure Pd. It is of interest to note that measurements made through application of the Haas–van Alphen effect [27], and later confirmed [28,29], show that there are actually ~ 0.36 electrons in the s-band of Au, or 0.36 holes in the Pd 4d-band, which roughly corresponds to the composition where the activation energy is at a minimum (65 at% Pd). Allison and Bond [9] review other reactions (such as benzene hydrogenation and formic acid decomposition) that experience the same type of effect in the activation energy with alloying as seen in this study.

The lowering of the activation energy with the addition of gold is only half of the total effect on the rate constant, since the presence of Au also decreases the pre-exponential factor, thereby decreasing the rate constant. The decrease in the pre-exponential factor corresponds to the dilution of the active Pd centers with Au. Of the five samples, the pure Pd catalyst has the highest pre-exponential factor (4.71×10^{16} cm^3/(g-Pd s)), while the 73 at% Pd catalyst has the lowest pre-exponential factor (5.59×10^6 cm^3/(g-Pd s)). Possible explanations of this include the presence of any long-range order at the surface, which might decrease the number of "ensembles" present, or their concentration among the grains in each particle. Another important effect of the addition of Au in forming an alloy with Pd is that Au inhibits hydride formation and thus decreases the hydrogen solubility.

Table 2
Kinetic and reaction data for the hydrogenation of 1,3-butadiene over the Pd–Au/SiO_2 catalysts [a]

Type	Surf. comp. (% Pd)	E_a (kcal/mol)	k_0 (cm^3/(g-Pd s))	k at 21°C (cm^3/(g-Pd s))	TOF at 21°C (s^{-1})	Conversion at 220°C
fabricated	44	8.34	4.22×10^7	28.8	12.1	0.50
fabricated	57	5.84	1.06×10^7	489.7	176.5	0.52
fabricated	73	6.52	5.59×10^6	84.9	23.2	0.46
fabricated	87	13.5	4.50×10^{12}	427.3	93.5	0.54
fabricated	100	20.0	4.71×10^{16}	67.5	8.40	0.61
thin film	54	5.97	3.60×10^5	14.4	5.63	–
thin film	76	6.38	3.94×10^5	2.17	2.17	–

[a] Reaction conditions: $P_{tot} = 1$ atm, $H_2/C_4H_6 = 125$, total flow = 110 cm^3/min.

This must affect the reaction kinetics, however a quantitative correlation of such an effect could not be obtained.

Regarding the possible effect of impurities such as S or C on the change of the activation energy, we did not detect sulfur before or after reaction. Carbon is present both before and after reaction, but because of the high H_2 to hydrocarbon ratio used, we do not expect carbon to be a major factor since no deactivation is detected with time on stream. The Pd thin films and microfabricated catalysts were prepared by exposure to similar environments during evaporation of Pd and Au except for the area exposed varied. We do not believe that the results reflects levels of impurities, but rather the effect of Au in Pd surface coverage and in changing the energetics of gas–surface interaction. The activation energy of Au should be larger than that of Pd. The Pd–Au bimetallic catalyst is not the simple addition of the two metals but it goes through a minimum between these two limits.

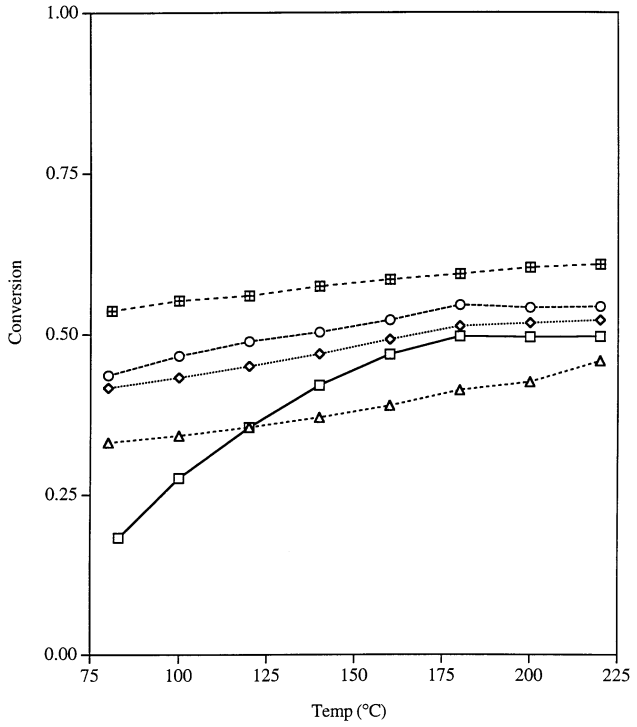

Figure 4. Conversion as a function of reaction temperature for the hydrogenation of 1,3-butadiene over Pd–Au/SiO_2 microfabricated catalysts: (□) 44 at% Pd, (◇) 57 at% Pd, (△) 73 at% Pd, (○) 87 at% Pd, (⊞) 100 at% Pd. Reaction conditions: $P_{tot} = 1$ atm, $H_2/C_4H_6 = 125$, total flow = 110 cm^3/min.

The selectivity of 1-butene (figure 5a) shows an increase with the addition of Au, but only at higher conversions (above 30%). For conversion levels below 30%, the pure Pd catalyst actually has a higher selectivity towards 1-butene than the bimetallic catalysts. The Pd catalyst reaches a maximum 1-butene selectivity of 96% near zero conversion and a minimum of 12% at approximately 50% conversion. All of the bimetallic catalysts display lower maximum and higher minimum in selectivity than the monometallic catalyst. At low conversions the bimetallic catalysts exhibit a 1-butene selectivity between 60 and 80% and at 50% conversion the selectivity lies between 25 and 60%. Conversely, the Pd catalyst is more selective towards butane (figure 5b) at higher conversions than the bimetallic catalysts; its greatest selectivity of 34% occurs at a conversion level of 55%. Figure 5c shows that the Pd catalyst is less selective towards trans-2-butene at low conversions than the bimetallic catalysts. The formation of cis-2-butene (figure 5d) is not significantly affected by the addition of gold at any conversion level.

Changes in selectivity with the addition of Au agree with the results presented by Miura et al. [25], where alloying was also confirmed. The addition of gold produces a catalyst that was more selective towards 1-butene at higher conversions (> 30%). Joice et al. [24] also report increases in 1-butene selectivity with the addition of Au, but only for the narrow composition range where they see an increase in activation energy. It is possible that the addition of Au decreases the adsorption of 1,3-butadiene and further hydrogenation of butene becomes less favorable. The reaction mechanism for the hydrogenation of 1,3-butadiene on a Pt catalyst, originally suggested by Phillipson et al. [30] and later supported by Pradier et al. [31], states that butane is formed by the hydrogenation of 1-butene and not the 2-

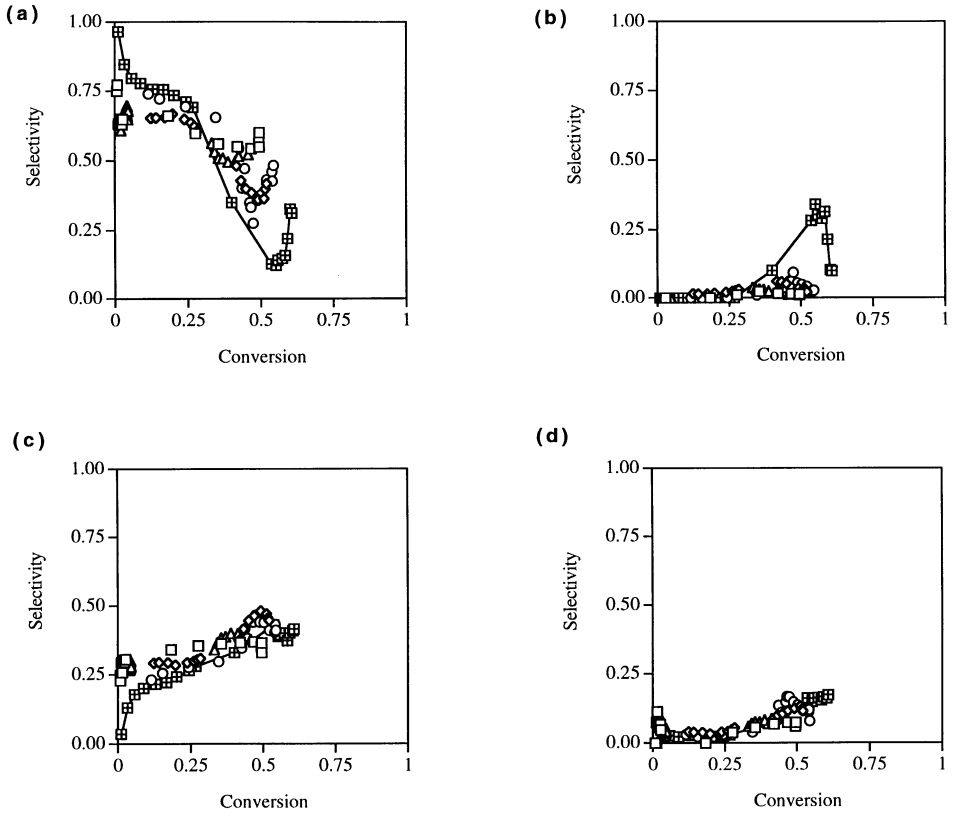

Figure 5. Selectivity of (a) 1-butene, (b) butane, (c) trans-2-butene, and (d) cis-2-butene as a function of conversion for the hydrogenation of 1,3-butadiene over Pd–Au/SiO_2 microfabricated catalysts; (□) 44 at% Pd, (◇) 57 at% Pd, (△) 73 at% Pd, (○) 87 at% Pd, (⊞) 100 at% Pd. Reaction conditions: $P_{tot} = 1$ atm, $H_2/C_4H_6 = 125$, total flow = 110 cm^3/min.

butenes. This is characterized by the inversely changing selectivity of 1-butene and butane as a function of conversion, along with the continual increase in both 2-butene selectivity. The data from our study suggest that this mechanism is also valid for the microfabricated catalysts.

The AFM images show that the surface of each Pd island, even though well defined in a 2D shape, is still very complex, and must be made smaller to extract the full advantage of microfabricating a catalyst. The main disadvantage of preparing the microfabricated catalysts via contact lithography was in the limitations imposed on the particle size. The incentive for reducing the particle size is to better mimic the crystallite sizes present in conventional supported catalysts used in industry and to control the morphology of the resulting island. One method for accomplishing this is to use electron beam lithography (EBL). Work done by the Electrical Engineering Department in the Microelectronics Laboratory at Notre Dame has demonstrated that Au dots of about 25 nm can be obtained using EBL [32]. Ribeiro and Somorjai [33] discussed a catalyst prepared using e-beam lithography with 50 nm Pt particles, indicating that it has been used for studies of CO oxidation and ethylene hydrogenation. Further refinements in the process and upgrades in technology should allow a reduction in this dimension. However, the main limitation in this process (EBL) is that with the current technology it takes a long time to generate the number of particles equivalent to the catalysts prepared via contact lithography. Refinements in the type of resist used and higher energy electron beams could also reduce the time required for exposure. Work is underway in our group to attain such sizes and achieve full control of size, composition and distribution of particles in a model catalyst and relate such variables to catalytic activity and selectivity.

4. Conclusions

Bimetallic Pd–Au microfabricated catalysts were prepared and compared to thin film samples of similar bulk composition. The microfabricated catalysts were more active than the thin film samples, because of differences in surface morphology. The thin film samples showed evidence of a high degree of sintering after pretreatment, unlike the microfabricated catalysts in which sintering did not occur. The main advantage of the bimetallic microfabricated catalysts is that the formation of a true alloy is guaranteed by the preparation process. The addition of Au to Pd lowered the activation energy, which

leads to an increase in the rate constant and TOF at low temperatures. At high temperatures the Pd catalyst is most active, presumably due to it having the largest number of surface sites, while the 73 at% Pd catalyst has the lowest conversion. The presence of Au also has an effect on the selectivity. At low conversions (less than 30%) the addition of gold suppresses the formation of 1-butene and increases the production of trans-2-butene, whereas at higher conversions the amount of 1-butene increases, while the amount of butane formed is diminished.

Acknowledgement

Financial support through NSF grants (NSF CTS 92-15339 and NSF ECS 92-53580-002) and the Graduate Assistance in Areas of National Need Program (GAANNP) through Notre Dame's Center for Bioengineering and Pollution Control is gratefully acknowledged. Furthermore, we would like to thank the National Nanofabrication Facility at Cornell for technical assistance and for supplying the photomasks.

References

[1] K. Foger, in: *Catalysis: Science and Technology*, Vol. 6, eds. J.R. Anderson and M. Boudart (Springer, New York, 1984) p. 228.
[2] E.E. Latta and H.P. Bonzel, in: *Interfacial Segregation*, eds. W.C. Johnson and J.M. Blakely (American Society for Metals, Metals Park, 1979) p. 381.
[3] S. Alerasool and R.D. Gonzalez, J. Catal. 124 (1990) 204.
[4] P. van Zant, *Microchip Fabrication: A Practical Guide to Semiconductor Processing*, 2nd Ed. (McGraw-Hill, New York, 1990) p. 11.
[5] P.T. Moseley and B.C. Tofield, *Solid State Gas Sensors* (Hilger, Philadelphia, 1987) p. 227.
[6] I. Zuburtikudis and H. Saltsburg, Science 258 (1992) 1337.
[7] A.C. Krauth, K.H. Lee, G.H. Bernstein and E.E. Wolf, Catal. Lett. 27 (1994) 43.
[8] D.D. Eley, J. Res. Inst. Catal. Hokkaido Univ. 16 (1968) 101.
[9] E.G. Allison and G.C. Bond, Catal. Rev. 7 (1972) 233.
[10] R.L. Moss and L. Whalley, Adv. Catal. 22 (1972) 115.
[11] J. Schwank, Gold Bull. 18 (1985) 2.
[12] H. Okamoto and T.B. Massalski, in: *Binary Alloy Phase Diagrams*, 2nd Ed., Vol. 1, ed. T.B. Massalski (ASM International, 1990) p. 409.
[13] G. Maire, L. Hilaire, F.G. Gault and A. O'Cinneide, J. Catal. 44 (1976) 293.
[14] B.J. Wood and H. Wise, Surf. Sci. 52 (1975) 151.
[15] Y.L. Lam and M. Boudart, J. Catal. 50 (1977) 530.
[16] D.F. Ollis, J. Catal. 59 (1979) 430.
[17] A. Jablonski, S.H. Overbury and G.A. Somorjai, Surf. Sci. 65 (1977) 578.
[18] D.D. Eley and P.B. Moore, J. Chem. Soc. Faraday I 76 (1980) 1388.
[19] K.H. Lee and E.E. Wolf, Catal. Lett. 26 (1994) 297.
[20] C.M. Pradier, E. Margot, Y. Berthier and J. Oudar, Appl. Catal. 43 (1988) 177.
[21] M. Primet, M. El Azhar and M. Guenin, Appl. Catal. 58 (1990) 241.
[22] B. Tardy, C. Noupa, C. Leclercq, J.C. Bertolini, A. Hoareau, M. Treilleux, J.P. Faure and G. Nihoul, J. Catal. 129 (1991) 1.
[23] A. Sarkany, Z. Zsoldos, B. Furlong, J.W. Hightower and L. Guczi, J. Catal. 141 (1993) 566.
[24] B.J. Joice, J.J. Rooney, P.B. Wells and G.R. Wilson, Disc. Faraday Soc. 41 (1966) 223.
[25] H. Miura, M. Terasaka, K. Oki and T. Matsuda, in: *New Frontiers in Catalysis*, Proc. 10th Int. Congr. on Catalysis, eds. L. Guczi, F. Solymosi and P. Tétényi (Elsevier, Amsterdam, 1993) p. 2379.
[26] J.C. Bertolini, P. Delichere, B.C. Khanra, J. Massardier, C. Noupa and B. Tardy, Catal. Lett. 6 (1990) 215.
[27] J.J. Vuillemin and M.G. Priestley, Phys. Rev. Lett. 14 (1965) 307.
[28] F.M. Meuller and M.G. Priestley, Phys. Rev. 148 (1966) 638.
[29] H. Kimura, A. Katsuki and M. Shimizu, J. Phys. Soc. Japan 21 (1966) 307.
[30] J.J. Phillipson, P.B. Wells and G.R. Wilson, J. Chem. Soc. (1969) 1351.
[31] C.M. Pradier, E. Margot, Y. Berthier and J. Oudar, Appl. Catal. 43 (1988) 177.
[32] G. Bazan and G.H. Bernstein, J. Vac. Sci. Technol. A 11 (1993) 1745.
[33] F.H. Ribeiro and G.A. Somorjai, Recl. Trav. Chim. Pays-Bas 113 (1994) 419.